Chapter 2

THREE-PHASE DIODE BRIDGE RECTIFIER

The subject of this book is reduction of total harmonic distortion (THD) of input currents in three-phase diode bridge rectifiers. Besides the reduction of the input current THD, the methods proposed here result in improvement of the rectifier power factor (PF). To build a foundation to introduce the new methods, in this chapter a three-phase diode bridge rectifier is analyzed and relevant voltage waveforms are presented and their spectra derived. Also, logic functions that define states of the diodes in the three-phase diode bridge, termed diode state functions, are defined.

Let us consider a three-phase diode bridge rectifier as shown in Fig. 2-1. The rectifier consists of a three-phase diode bridge, comprising diodes D1 to D6. In the analysis, it is assumed that the impedances of the supply lines are low enough to be neglected, and that the load current I_{OUT} is constant in time. The results and the notation introduced in this chapter are used throughout the book.

First, let us assume that the rectifier is supplied by a balanced undistorted three-phase voltage system, specified by the phase voltages:
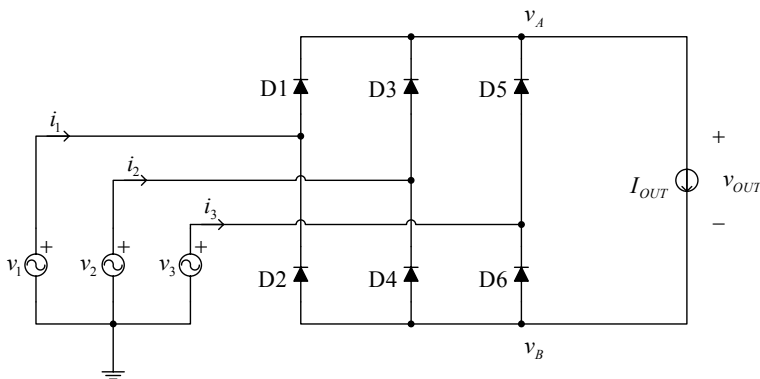

Figure 2-1. Three-phase diode bridge rectifier.

$$v_1 = V_m \cos(\omega_0 t), \tag{2.1}$$

$$v_2 = V_m \cos\left(\omega_0 t - \frac{2\pi}{3}\right), \tag{2.2}$$

and

$$v_3 = V_m \cos\left(\omega_0 t - \frac{4\pi}{3}\right). \tag{2.3}$$

The amplitude of the phase voltage V_m equals

$$V_m = V_{PRMS}\sqrt{2}\,, \tag{2.4}$$

where V_{PRMS} is the root-mean-square (RMS) value of the phase voltage. Waveforms of the input voltages are presented in Fig. 2-2.

Assuming that I_{OUT} is strictly greater than zero during the whole period, in each time point two diodes of the diode bridge conduct. The first conducting diode is from the group of odd-indexed diodes $\{D1, D3, D5\}$, and it is connected by its anode to the highest of the phase voltages at the time point considered. The second conducting diode is from the group of even-indexed diodes $\{D2, D4, D6\}$, and it is connected by its cathode to the lowest of the phase voltages. Since one phase voltage cannot be the highest and the lowest at the same time for the given set of phase voltages specified by (2.1), (2.2), and (2.3), two of the phases are connected to the load while one phase is unconnected in each point in time. This results in an input current equal to zero in the time interval when the phase voltage is neither maximal nor minimal. The gaps in the phase currents are the main reason for introducing the current injection methods, as they are analyzed in the next chapter.

The described operation of the diodes in the diode bridge results in a positive output terminal voltage equal to the maximum of the phase voltages, i.e.,

$$v_A = \max(v_1, v_2, v_3), \tag{2.5}$$

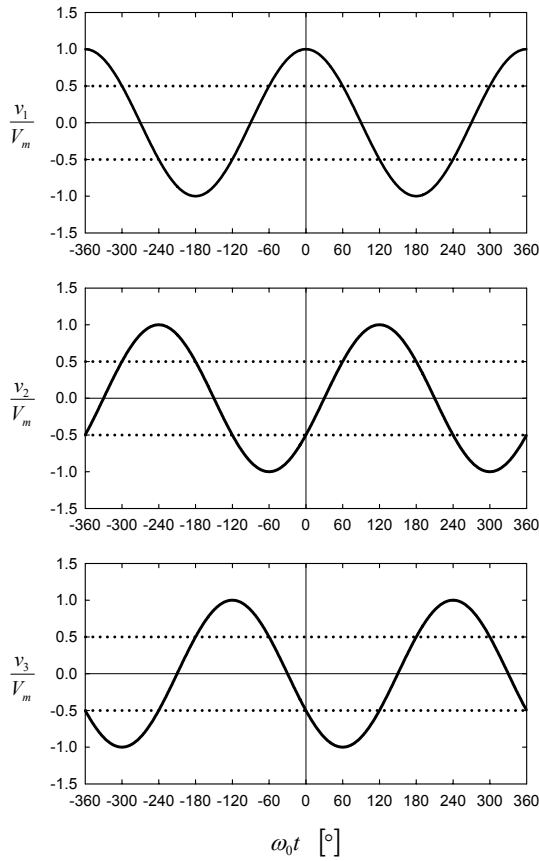while the voltage of the negative output terminal equals the minimum of the phase voltages,

Figure 2-2. Waveforms of the input voltages.

$$v_B = \min(v_1, v_2, v_3).$$ (2.6)

Waveforms of the output terminal voltages specified by (2.5) and (2.6) are presented in Fig. 2-3. These waveforms are periodic, with the period equal to one third of the line period; thus their spectral components are located at triples of the line frequency. Fourier series expansion of the waveform of the positive output terminal leads to

$$v_A = \frac{3\sqrt{3}}{\pi} V_m \left(\frac{1}{2} + \sum_{n=1}^{+\infty} \frac{(-1)^{n+1}}{9n^2 - 1} \cos(3n\omega_0 t) \right),$$ (2.7)
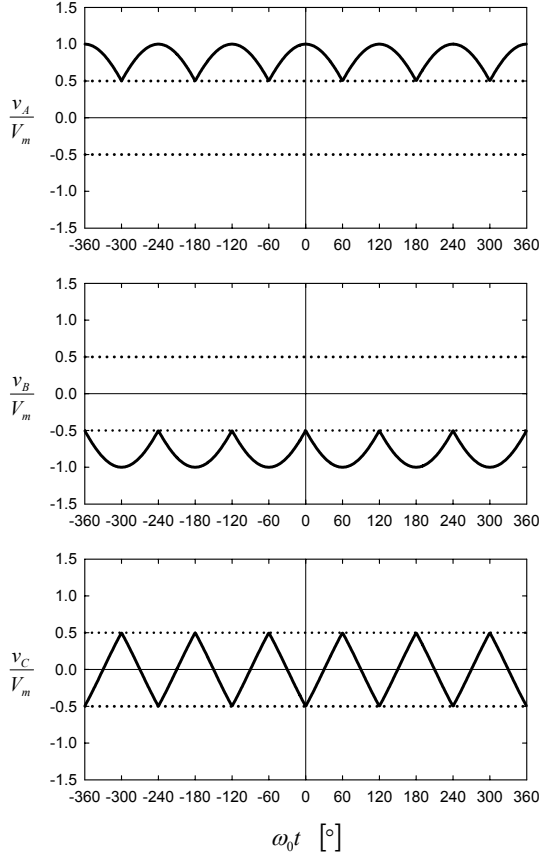
Figure 2-3. Waveforms of the output terminal v_A and v_B, and the waveform of v_C.

while the Fourier series expansion of the voltage of the negative input terminal results in

$$v_B = \frac{3\sqrt{3}}{\pi} V_m \left(-\frac{1}{2} + \sum_{n=1}^{+\infty} \frac{1}{9n^2 - 1} \cos(3n\omega_0 t) \right).$$
(2.8)

These Fourier series expansions are used frequently in analyses of various current injection methods. Some useful properties of the Fourier series expansions of the output terminal voltages should be underlined here. First, both Fourier series expansions contain spectral components at multiples of tripled line frequency, i.e., at triples of the line frequency. The corresponding spectral components of v_A and v_B at odd triples of the line frequency at

$3(2k-1)\omega_0$, where $k \in N$, are the same, having the same amplitudes and the same phases. On the other hand, the corresponding spectral components at even triples of the line frequency, at $6k\omega_0$, have the same amplitudes, but opposite phases. These properties are used in the design of current injection networks described in Chapters 6 and 8.

   The diode bridge output voltage is given by

$$v_{OUT} = v_A - v_B,$$ (2.9)

and its waveform is presented in Fig. 2-4. The Fourier series expansion of the output voltage is

$$v_{OUT} = \frac{3\sqrt{3}}{\pi} V_m \left(1 - \sum_{k=1}^{+\infty} \frac{2}{36k^2 - 1} \cos(6k\omega_0 t) \right).$$ (2.10)

Since spectra of v_A and v_B have the same spectral components at odd triples of the line frequency, these spectral components cancel out in the spectrum of the output voltage. Thus, the spectrum of the output voltage contains spectral components only at sixth multiples of the line frequency. The DC component of the output voltage equals

$$V_{OUT} = \frac{3\sqrt{3}}{\pi} V_m \approx 1.65 V_m \approx 2.34 V_{PRMS},$$ (2.11)

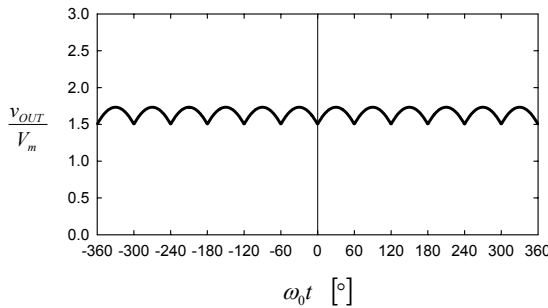while the Fourier series expansion of the AC component of the output voltage is

Figure 2-4. Waveform of the output voltage.

$$\hat{v}_{OUT} = -\frac{3\sqrt{3}}{\pi}V_m \sum_{k=1}^{+\infty}\frac{2}{36k^2-1}\cos(6k\omega_0 t). \tag{2.12}$$

Another waveform of interest in the analyses that follow is the waveform of "the remaining" voltage, v_C, i.e., the waveform obtained from segments of the phase voltages during the time intervals when they are neither maximal nor minimal. A node in the circuit of Fig. 2-1 where that voltage could be measured does not exist, in contrast to the waveforms of v_A and v_B that can be observed at the diode bridge output terminals. However, the waveform and the spectrum of v_C can be computed easily using the fact that the sum of the instantaneous values of the phase voltages equals zero,

$$v_1 + v_2 + v_3 = 0. \tag{2.13}$$

In each point in time, one of the phase voltages equals v_A, another one equals v_B, while the remaining one equals v_C. Thus, the output terminal voltages and "the remaining voltage" add up to zero. This gives the following expression for "the remaining voltage":

$$v_C = -v_A - v_B, \tag{2.14}$$

and its spectrum is computed using spectra of v_A and v_B, given by (2.7) and (2.8), resulting in

$$v_C = -\frac{3\sqrt{3}}{\pi}V_m \sum_{k=1}^{+\infty}\frac{2}{(6k-3)^2-1}\cos((6k-3)\omega_0 t). \tag{2.15}$$

In the spectrum of "the remaining voltage" the spectral components are located at odd triples of the line frequency, since the spectral components of v_A and v_B at even triples of the line frequency cancel out.

Another voltage of interest is the average of the output terminal voltages, defined as

$$v_{AV} = \frac{1}{2}(v_A + v_B) = -\frac{1}{2}v_C. \tag{2.16}$$

Using the spectrum of v_C, given by (2.15), the spectrum of v_{AV} is obtained as

$$v_{AV} = \frac{3\sqrt{3}}{\pi} V_m \sum_{k=1}^{+\infty} \frac{1}{(6k-3)^2 - 1} \cos((6k-3)\omega_0 t). \tag{2.17}$$

The spectral components of v_{AV} are located at odd triples of the line frequency, the same as in the spectrum of v_C.

After the waveforms of the rectifier voltages are defined and their spectra derived, waveforms of the rectifier currents are analyzed. In the analysis of the rectifier currents, let us start from the states of the diodes. First, let us define the diode state functions d_k for $k \in \{1,2,3,4,5,6\}$ such that $d_k = 1$ if the diode indexed with k conducts, and $d_k = 0$ if the diode is blocked. Values of the diode state functions are summarized in Table 2-1, while the waveforms of the diode state functions during two line periods are depicted in Fig. 2-5. From the data of Table 2-1 it can be concluded that the rectifier of Fig. 2-1 can be analyzed as a periodically switched linear circuit, since the states of the diodes are expressed as functions of the time variable. This significantly simplifies the analysis, as seen in Chapter 9, where the discontinuous conduction mode of the diode bridge is analyzed, though with significant mathematical difficulties, since the circuit cannot be treated as a periodically switched linear circuit.

After the diode state functions are defined, currents of the diodes can be expressed as

$$i_{Dk} = d_k(\omega_0 t) I_{OUT} \tag{2.18}$$

for $k \in \{1,2,3,4,5,6\}$. All of the diode current waveforms have the same average value:

$$I_D = \frac{1}{3} I_{OUT}, \tag{2.19}$$

Table 2-1. Diode state functions.

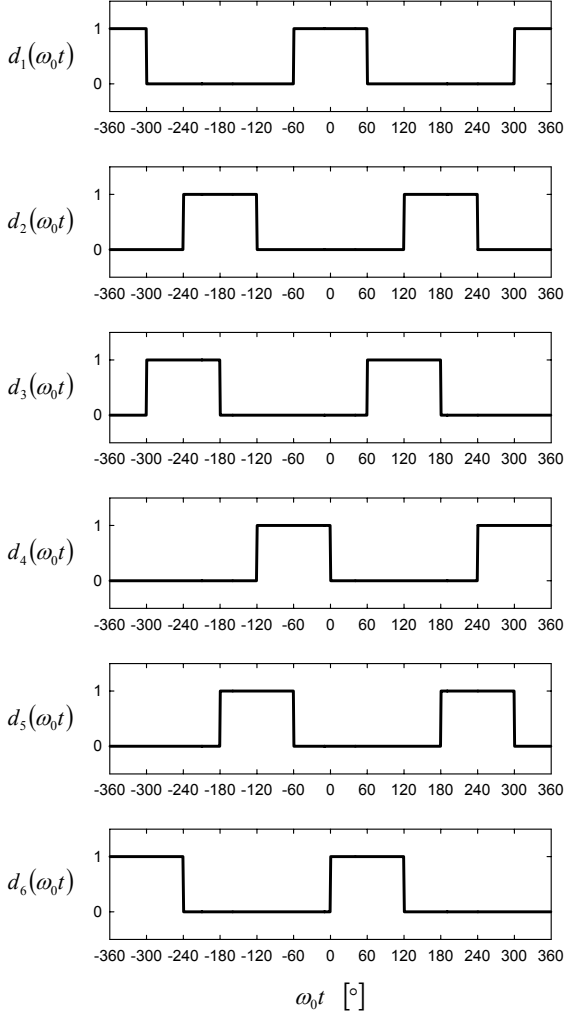| Segment	$d_1(\omega_0 t)$	$d_2(\omega_0 t)$	$d_3(\omega_0 t)$	$d_4(\omega_0 t)$	$d_5(\omega_0 t)$	$d_6(\omega_0 t)$
$0 < \omega_0 t < 60°$	1	0	0	0	0	1
$60° < \omega_0 t < 120°$	0	0	1	0	0	1
$120° < \omega_0 t < 180°$	0	1	1	0	0	0
$180° < \omega_0 t < 240°$	0	1	0	0	1	0
$240° < \omega_0 t < 300°$	0	0	0	1	1	0
$300° < \omega_0 t < 360°$	1	0	0	1	0	0

Figure 2-5. Waveforms of the diode state functions.

which is of interest for sizing the diodes. The maximum of the reverse voltage that the diodes are exposed to is equal to the maximum of the output voltage and equal to the line voltage amplitude,

$$V_{D\max} = V_m \sqrt{3} = V_{PRMS} \sqrt{6} \, . \tag{2.20}$$

Using the diode state functions, the rectifier input currents i_p, where

$p \in \{1, 2, 3\}$, can be expressed as

$$i_p = I_{OUT} \left(d_{2p-1}(\omega_0 t) - d_{2p}(\omega_0 t) \right). \tag{2.21}$$

Waveforms of the input currents are presented in Fig. 2-6. The input currents have the same RMS value, equal to

$$I_{RMS} = \frac{\sqrt{6}}{3} I_{OUT}. \tag{2.22}$$
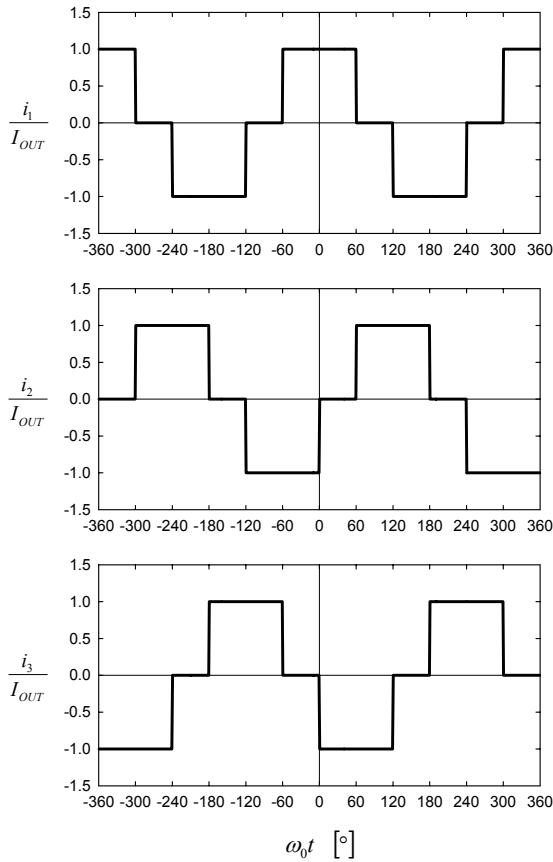
The output power of the rectifier is

Figure 2-6. Waveforms of the input currents.

$$P_{OUT} = V_{OUT}I_{OUT} = \frac{3\sqrt{3}}{\pi}V_m I_{OUT} = P_{IN} \qquad (2.23)$$

and it is the same as the input power P_{IN}, since losses in the rectifier diodes are neglected in the analysis and there are no other elements in the circuit of Fig. 2-1. The apparent power observed at the rectifier input is

$$S_{IN} = 3V_{PRMS}I_{RMS} = \sqrt{3}V_m I_{OUT}. \qquad (2.24)$$

From the rectifier input power given by (2.23) and the rectifier apparent power given by (2.24), the power factor at the rectifier input is obtained as

$$PF = \frac{P_{IN}}{S_{IN}} = \frac{3}{\pi} = 0.9549. \qquad (2.25)$$

This value for the power factor is reasonably good, and satisfies almost all of the power factor standards. It is significantly better than the power factor value of the rectifier with the capacitive filter connected at the output, which forces the rectifier to operate in the discontinuous conduction mode. The result is also good in comparison to single-phase rectifiers. Thus, the power factor value of (2.25) is not something to worry about. The parameter of the rectifier of Fig. 2-1 on which attention is focused is total harmonic distortion (THD) of the input currents.

To compute the THD values of the input currents, the RMS value of the input current fundamental harmonic is determined as

$$I_{1RMS} = \frac{\sqrt{6}}{\pi}I_{OUT}. \qquad (2.26)$$

The fundamental harmonics of the input currents are displaced to the corresponding phase voltages for

$$\varphi_1 = 0, \qquad (2.27)$$

which results in the displacement power factor (DPF):

$$DPF = \cos\varphi_1 = 1. \qquad (2.28)$$

The THD of the input currents is determined applying

$$THD = \frac{\sqrt{I_{RMS}^2 - I_{1RMS}^2}}{I_{1RMS}}, \tag{2.29}$$

resulting in

$$THD = \frac{1}{3}\sqrt{\pi^2 - 9} = 31.08\%. \tag{2.30}$$

This THD value is considered relatively high, and its reduction is of interest in some applications. Efficient methods to reduce the THD value of the input currents in three-phase diode bridge rectifiers are the topic of this book.

Some standards limit amplitudes of particular harmonic components of the input currents. Thus, the spectrum of the input currents is a topic of interest. The input currents can be expressed by Fourier series expansions of the form

$$i(t) = I_{DC} + \sum_{n=1}^{+\infty}\left(I_{C,n}\cos(n\omega_0 t) + I_{S,n}\sin(n\omega_0 t)\right)$$

$$= I_{DC} + \sum_{n=1}^{+\infty} I_n \cos(n\omega_0 t - \varphi_n), \tag{2.31}$$

where

$$I_{DC} = \frac{1}{2\pi}\int_{-\pi}^{\pi} i(t)\,d(\omega_0 t), \tag{2.32}$$

$$I_{C,n} = \frac{1}{\pi}\int_{-\pi}^{\pi} i(t)\cos(n\omega_0 t)\,d(\omega_0 t), \tag{2.33}$$

$$I_{S,n} = \frac{1}{\pi}\int_{-\pi}^{\pi} i(t)\sin(n\omega_0 t)\,d(\omega_0 t), \tag{2.34}$$

$$I_n = \sqrt{I_{C,n}^2 + I_{S,n}^2}, \tag{2.35}$$

and

$$\tan\varphi_n = \frac{I_{S,n}}{I_{C,n}}. \tag{2.36}$$

In the case of the input current of the first phase, specified by (2.21) for $p = 1$, the harmonic components are

$$I_{1,DC} = 0, \tag{2.37}$$

$$I_{1,C,n} = \frac{2}{\pi n}\left(\sin\frac{2\pi n}{3} + \sin\frac{\pi n}{3}\right)I_{OUT}, \tag{2.38}$$

$$I_{1,S,n} = 0; \tag{2.39}$$

thus

$$I_{1,n} = \frac{2}{\pi n}\left|\sin\frac{2\pi n}{3} + \sin\frac{\pi n}{3}\right|I_{OUT} \tag{2.40}$$

and

$$\varphi_n = \frac{\pi}{2}\left(1 - \mathrm{sgn}\left(\sin\frac{2\pi n}{3} + \sin\frac{\pi n}{3}\right)\right). \tag{2.41}$$

Waveforms of the input currents of the remaining two phases of the rectifier are displaced in phase for $2\pi/3$ in comparison to one to another, according to

$$i_1(\omega_0 t) = i_2\left(\omega_0 t - \frac{2\pi}{3}\right) = i_3\left(\omega_0 t + \frac{2\pi}{3}\right). \tag{2.42}$$

Thus, all of the input currents share the same amplitude spectrum but have different phase spectra, as can be derived by applying the time-displacement property for the Fourier series expansions in complex form.

To illustrate the operation of the diode bridge rectifier and to compare its real operation with the derived model, waveforms of an experimental rectifier are recorded and presented. The experimental rectifier operates with a phase voltage RMS value of $V_{PRMS} = 100$ V, corresponding to the input voltage amplitude of $V_m = 140$ V. The output current range is $0 < I_{OUT} < 10$ A, resulting in an output power of up to 2.5 kW. Experimentally recorded waveforms of the phase voltages, accompanied by the input currents, are presented in Fig. 2-7. From the waveforms, it can be concluded that the voltage system is balanced, but the voltages are slightly distorted in the form of two typical deviations: flattened sinusoid tops and notches. The flattened tops of the waveforms are caused primarily by single-phase rectifiers with capacitive filtering, typical for electronic equipment, and this type of distortion is not caused by the analyzed rectifier. However, the notches are caused by the nonzero line impedance and commutations in the diode bridge. This commutation effect can also be observed in a finite slope of the input current waveforms during the rising and falling edges, coinciding with the notches in the corresponding phase voltages.

Waveforms of the output voltage and the output current are presented in the bottom row of Fig. 2-7. The voltage waveform is different from the waveform presented in Fig. 2-4 around the minimums of the voltage, due to the notches in the phase voltages. Again, this effect is caused by nonzero impedance of the supply lines. In the output current waveform, the output current ripple at the sixth multiple of the line frequency can be observed. This ripple slightly affects the input current waveforms.

To illustrate dependence of the input voltage and the input current waveforms on the output current, and to determine limits of the accepted rectifier model, waveforms of the phase voltage and the input current are presented in Fig. 2-8 for $I_{OUT} = 4$ A, $I_{OUT} = 7$ A, and $I_{OUT} = 10$ A. The first effect to be observed is an increase in the duration of the notches at the phase voltage waveform by increases of the output current, caused by finite impedance of the supply lines. The second effect is increased output current ripple at $I_{OUT} = 10$ A, which is caused by saturation of the filter inductor core. Other than these two effects that are not captured by the accepted rectifier model, the rectifier behavior is within expected limits. In Table 2-2, dependence of the THD of the input voltage, THD of the input current, the input power, the apparent power at the rectifier input, and the rectifier power factor are presented. The voltage waveform is moderately distorted, which slightly increases the output current, due to the increased duration of the notches. The input current THD is slightly lower than predicted by (2.30), which is caused by the nonzero impedance of the supply lines. This
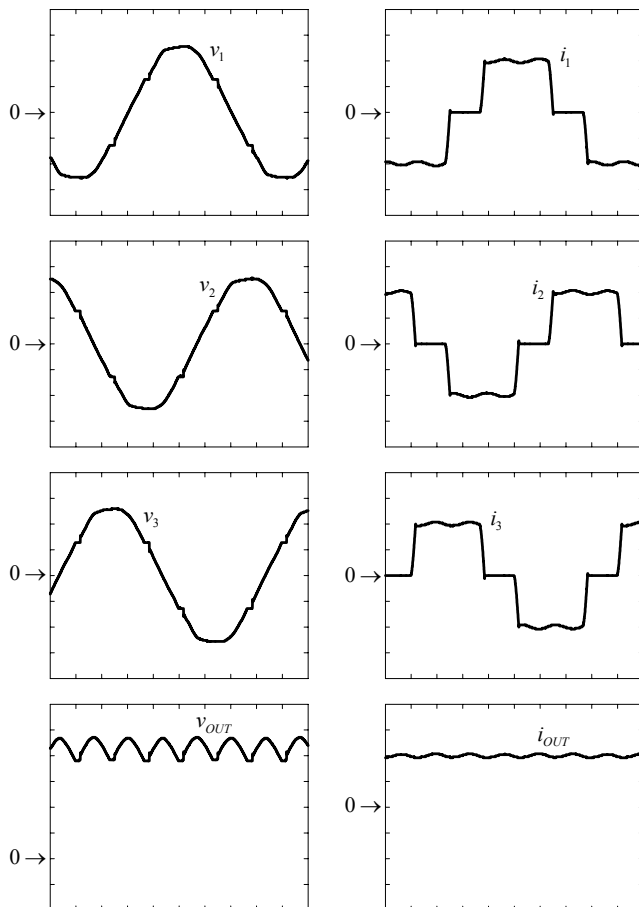
Figure 2-7. Experimentally recorded waveforms of the input voltages, the input currents, the output voltage, and the output current. Voltage scale = 50 V/div. Current scale = 5 A/div. Time scale = 2.5 ms/div.

impedance slightly smoothens the input current waveform during the diode state transitions, resulting in a lower THD. The power factor at the rectifier input is close to the expected value, given by (2.25).

From the experimental data it can be concluded that the rectifier model adequately describes the rectifier operation. However, the supply line
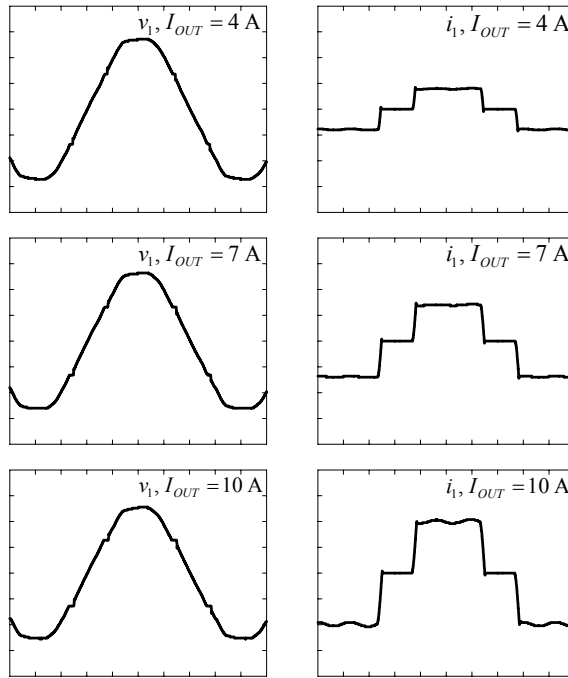
Figure 2-8. Experimentally recorded waveforms of the phase voltage and the input current for $I_{OUT} = 4$ A , $I_{OUT} = 7$ A , and $I_{OUT} = 10$ A . Voltage scale = 50 V/div. Current scale = 5 A/div. Time scale = 2.5 ms/div.

Table 2-2. Dependence of the rectifier parameters on I_{OUT} .

I_{OUT}	$THD(v_1)$	$THD(i_1)$	P_{IN}	S_{IN}	PF
4 A	3.17 %	29.47 %	909.8 W	946.8 VA	0.9610
7 A	3.34 %	28.65 %	1544.3 W	1607.8 VA	0.9605
10 A	3.42 %	27.94 %	2121.0 W	2212.1 VA	0.9588

inductance and the output current ripple might slightly affect the rectifier operation, and these phenomena are not included in the rectifier model. Application of the current injection methods will remove the notches from the phase voltages and make the inductance of the supply lines irrelevant. Thus, the output current ripple will remain the only parasitic effect to be concerned about.